

# Lattice animals and the Percolation model under rotational constraint

Indrani Bose

Department of Physics  
Bose Institute  
93/1, A. P. C. Road  
Calcutta-700 009, India.

## Abstract

The effect of rotational constraint on the properties of lattice models like the self-avoiding walk, lattice animals and percolation is discussed. The results obtained so far, using a variety of exact and approximate techniques, are described. Examples of the rotational constraint in real systems are also given.

## I. Introduction

Lattice models describe a wide variety of physical, chemical and biological systems. The systems either have an underlying lattice structure or are studied on a lattice for convenience. In the latter case, only those properties of the system are studied which are independent of the microscopic structural details of the system. In this article, we will discuss three lattice models: the self-avoiding walk (SAW), lattice animal (LA), and percolation. We will mainly discuss the effect of rotational constraint on the various configurational and connectivity properties of the models.

A SAW is a walk on a lattice with the constraint that a site once visited cannot be visited again. The SAW is a model of linear polymers in dilute solution [1]. A linear polymer can be pictured as a string of smaller chemical units called monomers. There is a one-to-one correspondence between each possible configuration of the polymer and a particular SAW on the lattice. The self-avoidance criterion is due to the excluded-volume effect of polymers which implies that no two monomers can occupy the same physical space.

LAs are clusters of connected sites (site LA) or bonds (bond LA) embedded in a lattice. The LAs represent random clusters which can occur in a

variety of systems. In terms of polymers, one example is branched polymers in dilute solution. The percolation model is a model of disorder and has, in general, two versions, site and bond. In the site (bond) percolation model, the probability that a site (bond) of the lattice is occupied is  $p$ . For  $p$  less than a critical value  $p_c$ , called the percolation threshold, no extended network of sites (bonds) spans the lattice. For  $p \geq p_c$ , such a network exists with probability one. The percolation threshold  $p_c$  has a unique value for an infinitely large lattice. The value of  $p_c$  is different for different lattices. The percolation transition at  $p = p_c$  is a phase transition, often called a geometrical phase transition. In one phase ( $p < p_c$ ), an infinite cluster exists and in the other phase ( $p \geq p_c$ ), there is no infinite cluster. In the vicinity of  $p = p_c$ , the percolation model exhibits critical phenomena analogous to those exhibited by a second-order thermodynamic phase transition. The percolation model has extensive applications in physics, chemistry and biology [2, 3, 4, 5].

We now show the connection between LAs and the percolation problem. We consider the site cluster problem. The generating function describing an ensemble of clusters of all sizes is written as

$$G(x, y) = \sum_{s,t} g_{s,t} x^s y^t \quad (1)$$

$g_{s,t}$  is the number of distinct LAs of size  $s$  and  $t$  perimeter sites, each animal being weighted by a factor  $x^s y^t$ . The size  $s$  of the animal is equal to the number of sites in the cluster. In the percolation problem, each cluster site is occupied with probability  $p$  and a perimeter site being an unoccupied site has the probability  $1-p$  of being so. Thus  $x = p$  and  $y = 1-p$  in Eq.(1). The corresponding generating function is

$$\begin{aligned} G(p, q) &= \sum_{s,t} g_{s,t} p^s q^t \\ &= \sum_s D_s(q) p^s \end{aligned} \quad (2)$$

where  $q = 1-p$  and  $D_s(q) = \sum_t g_{s,t} q^t$ . The  $D_s(q)$  are known as perimeter polynomials. For LAs, clusters of the same size have equal weight irrespective of the number of perimeter sites, so  $y = 1$  in Eq.(1) and the generating function becomes

$$G(x, 1) = \sum_s g_s x^s \quad (3)$$

where  $g_s = \sum_t g_{s,t}$  is the total number of clusters of size  $s$ . Eq.(2) shows that percolation and LA models are related through the perimeter polynomials construction of which requires knowledge of LA numbers. Both generating functions (2) and (3) become singular as  $p \rightarrow p_c$  and  $x \rightarrow x_c$ , respectively, hence  $p_c$  and  $x_c$  are identified as critical points of the respective ensembles of clusters. Below the critical point small clusters are predominant in number, above the critical point the reverse situation is true. At the critical point, clusters of all sizes exist, a familiar characteristic of critical phenomena. In fact, the transition is a second-order transition and the generating function in each case plays the role of free energy in thermal critical phenomena. Analogous to thermodynamic quantities, cluster-related quantities can be defined for the geometric models. These show singular behaviour as the critical point is being reached. The singularity is of the power-law type with an associated critical exponent. For the SAW model, a generating function similar to Eq.(3) can be defined with  $s$  being the number of steps in the walk. For generating functions of the type (3), it can be shown [6] that every critical exponent characterising a singularity as  $x \rightarrow x_c$ , say, is uniquely related to a critical exponent along the path  $s \rightarrow \infty$ , i.e.,  $s \sim |x - x_c|^{-1}$ . In the asymptotic limit of  $s$  going to infinity, various walk or cluster properties scale with size. We will now describe two such relations for site LAs. Equivalent relations can be written down for SAWs. The first relation shows that the total animal (cluster) number  $g_s$  scales as

$$g_s \sim_{s \rightarrow \infty} \lambda^s s^{-\theta} \quad (4)$$

where  $\lambda$  is a constant for a particular lattice and is known as the ‘growth parameter’ because asymptotically  $g_s / g_{s-1} \rightarrow \lambda$ . The parameter  $\theta$  (critical exponent) is ‘universal’ in the sense that it has the same value for all lattices in dimension  $d$ , the value changes only if  $d$  changes. The second quantity we are interested in is the average radius of gyration defined as  $R_s = (\sum_{i=1}^s r_i^2 / s)^{1/2}$  where  $r_i$  is the distance of a cluster site  $i$  from the centre of mass of the cluster and  $\langle \dots \rangle$  denotes average over all animals. As  $s \rightarrow \infty$ ,  $R_s$  scales with  $s$  as

$$R_s \sim s^\nu \quad (5)$$

where  $\nu$  is another critical exponent. In connection with relations like (4) and (5), it has been shown[5] that LAs and large clusters below the percolation threshold have identical scaling behaviour. For the SAW model,  $g_s$  is the

number of distinct SAWs with  $s$  steps and  $R_s$  is the root-mean-square end-to-end displacement for walks with  $s$  steps.

The scaling relations (4) and (5) have been well-studied for both undirected and directed models. In the case of undirected SAW and LA, there is no constraint on connectivity. In the case of directed SAW and LA, there is a global directionality constraint. To give an example, starting from the origin and while occupying new sites, the animal can grow only upwards and towards the right. The undirected and directed lattice models are known to belong to different universality classes, i.e., the exponents  $\theta$  and  $\nu$  have different values. A new type of constraint [7, 8, 9, 10] that has been proposed is the rotational constraint. In the presence of this constraint, a SAW or a LA can grow either in the same direction as it has been growing in or in a specific rotational direction, say, clockwise. Similar constraint can also be defined for the percolation model. In Section II, the SAW model under rotational constraint, termed the spiral SAW (SSAW), is described. In Section III, spiral LAs are considered. A brief description is also given of directed compact site LAs for which the generating function can be determined in an exact manner. In Section IV, the spiral percolation model is discussed. Section V contains some concluding remarks.

## II. Spiral SAW

The model was first considered by Privman[7]. Let us consider the SSAW problem on a square lattice. Each step of the walk may either point in the same direction as the preceding one or in a direction rotated by  $+\pi/2$  w.r.t. it. The global behaviour arising from the two constraints of self-avoidance and the bond angle restrictions is quite novel. In general, a SSAW consists of an outward spiralling part and an inward spiralling part (Fig.1). Each SAW is composed of horizontal and vertical segments. Let  $s_n$  be the number of  $n$ -step SSAWs. In the asymptotic limit, exact, analytical expressions for  $s_n$  have been determined [11, 12, 13, 13, 14] in the cases of both the square and triangular lattices. We describe briefly the results obtained in Refs. [12-13] for the square lattice.

Let the first step of the walk be vertically upwards. Each SSAW can be decomposed into a concatenation of two walks of type I and C by either a vertical line (Fig.2(a)), a horizontal line (Fig.2(b)) or in some cases both

(Fig.2(c)).  $I_n$  denotes the set of  $n$ -step SSAWs whose last and third last segments are of equal length,  $i_n$  is the number of such walks.  $C_n$  is the set of  $n$ -step SSAWs whose last segment is at least one greater than the length of the third last segment and  $c_n$  the number of such walks. From Figs. 2(a) - 2(c), the section of the spiral from O to A belongs to  $I_k$  and that from A to N belongs to  $C_{n-k}$ . The walks of the type shown in Figs. 2(a) - 2(b) can be uniquely decomposed in this way. Thus

$$S_n = \sum_{k=0}^{n-1} i_k c_{n-k} - \sum_{k=1}^{n-1} i_k i_{n-k} \quad (6)$$

with  $i_0 = 1$ ,  $c_0 = 0$ ,  $c_1 = 1$ . The second sum corrects for a double-counting of walks of the type 2(c) by the first sum. A geometrical construction[12] transforms walks of the type 2(c) into two connected walks from the set I. The walk in the set  $C_{n+1}$  can be obtained by adding a step in a particular direction to each member of  $C_n \cup I_n$ . Thus

$$c_{n+1} = c_n + i_n \quad (7)$$

Now  $c_n$  is equal to the number of partitions of the integer  $n$ . An example is given in Fig.(3). Fig.3(a) represents a particular partition of the number 12. A line at  $45^\circ$  divides the set of points into two classes, representing vertical and horizontal segments. There are two horizontal segments of length 2 and 3 and two vertical segments of length 3 and 4. The resultant SSAW is shown in Fig.3(b). Each partition of the integer 12 can be represented by a pattern of points and each such pattern can be uniquely represented by a SSAW. All the spiral walks in the set  $C_n$  can be enumerated in this way.

Asymptotic expressions ( $n \rightarrow \infty$ ) for the number of partitions of integers are known from the classic work of Hardy and Ramanujan[15]. One obtains

$$c_n = \frac{1}{4\sqrt{3}n} e^{\pi(\frac{2n}{3})^{\frac{1}{2}}} \left[ 1 + \frac{c}{\sqrt{n}} + O\left(\frac{1}{n}\right) \right] \quad (8)$$

where  $c$  is a constant which can be determined. From (7),

$$i_n = \frac{\pi}{12\sqrt{2}n^{\frac{3}{2}}} e^{\pi(\frac{2n}{3})^{\frac{1}{2}}} \left[ 1 + O\left(\frac{1}{\sqrt{n}}\right) \right] \quad (9)$$

Substituting (8) and (9) into (6), one finds that the largest terms in the sum are in the vicinity of  $k = n/2$ . Expanding around the maximum and replacing the sum by an integral, one finally obtains

$$s_n = \left( \frac{\pi}{4 \times 3^{\frac{5}{4}}} \right) n^{\frac{-7}{4}} \exp[2\pi \left( \frac{n}{3} \right)^{\frac{1}{2}}] \left[ 1 + O\left( \frac{1}{\sqrt{n}} \right) \right] \quad (10)$$

Joyce[16] has obtained the complete asymptotic expansion for  $s_n$ . Lin[14] has obtained an expression for  $s_n$  in the case of the triangular lattice. By comparing the expression (10) with that (Eq.(4)) valid for undirected and directed SAWs, one finds that the rotational constraint produces a new scaling form for the number of SAWs. Blöte and Hilhorst[11] have also obtained an asymptotic form for the root mean square end-to-end distance of SSAWs. Again, the rotational constraint has a non-trivial effect on the scaling form.

### III. Spiral site lattice animals

Two versions of the spiral LA have been studied : ‘rooted’, i.e., the origin from which the animal is grown is kept fixed and ‘unrooted’, i.e., the origin is not specified. In the latter case, two animals differing only in the choice of the origin are considered identical. The number of distinct rooted animals of a certain size is much greater than the number of unrooted animals of the same size. Bose and Ray[9] have defined unrooted spiral LAs in  $d = 2$  to be a subset of undirected and unrooted LAs with the proviso that there is a site of the cluster, namely, the origin to which every other site of the cluster is connected through at least one spiral path. In a spiral path, connection is either in the forward direction or in a specific rotational direction, say, clockwise. An example of a spiral site LA is shown in Fig.4. In dimension  $d \geq 2$ , a possible definition of the spiral constraint is: the projection of the path joining any site of the animal to the origin (the first site to be occupied), on any specified plane, say the  $xy$  plane, should have no anticlockwise turns. Other definitions of the spiral constraint have also been suggested[10].

A variety of techniques can be used to study the configurational properties of LAs. For spiral LAs, the method of exact enumeration of clusters upto a certain size has been used to obtain the values of  $\lambda$  and the exponents  $\theta$  and  $\nu$  in the scaling relations (4) and (5). Unlike in the case of SSAWs, the scaling relations (4) and (5) appear to give an adequate description of the

configurational properties of spiral LAs. The exact enumeration of animals of a certain size  $s$  is done on the computer using the well-known Martin's algorithm[17]. This algorithm generates undirected LAs and then each animal is checked for spiral connection. Knowledge of LA numbers of various sizes enables one to calculate the ratios  $g_{s+1}/g_s$  for various values of  $s$ . From Eq.(4), in the large  $s$  limit, the plot of the ratio  $g_{s+1}/g_s$  versus  $1/s$  is that of a straight line. From the intercept and slope of the straight line, the growth parameter  $\lambda$  and the exponent  $\theta$  can be determined. For spiral site LAs on the square lattice, exact enumeration data is available for size upto  $s = 15$ [18]. The values of  $\lambda$  and  $\theta$  are determined as  $\lambda = 3.002 \pm 0.020$  and  $\theta = 0.69 \pm 0.10$ . The radius-of-gyration exponent  $\nu = 0.50 \pm 0.02$ , i.e., the LAs are nearly-compact. These values are different from the corresponding values in the cases of undirected and directed LAs. Thus spiral LAs belong to a new universality class.

For the undirected and directed LAs, it is well-known that animals and trees (animals without loops) belong to the same universality class, i.e., loops have no effect on cluster statistics. This fact has been arrived at through detailed studies using techniques like both field-theoretic and position space RG, series-expansion and Monte Carlo enumeration[19, 20, 21, 22]. For spiral trees, the values of  $\lambda_0$ ,  $\theta_0$  and  $\nu_0$  have been obtained as[18] (from exact enumeration data upto  $s = 15$ )  $\lambda_0 = 2.123 \pm 0.004$ ,  $\theta_0 = -1.318 \pm 0.020$  and  $\nu_0 = 0.67 \pm 0.02$ . These values are different from the corresponding values for spiral LAs. Thus the spiral LAs and trees belong to different universality classes, i.e., loops have a non-trivial effect on spiral animal statistics. It has as yet not been possible to rigorously explain this fact but a special feature of spiral clusters is worth mentioning. For both ordinary and directed animals, an animal with loops becomes a tree as soon as a minimal number of bonds (for bond LAs) or sites (for site LAs) are removed but this is not always the case for a spiral animal. A tree obtained from a spiral animal with loops need not be a spiral tree. Also, in order to grow in the forward direction, a spiral animal should contain many loops. Without the loops, spiral connectivity is not possible in many cases. How these facts affect asymptotic cluster characteristics is still not understood.

An interesting result associated with the LA problem is that of dimensional reduction. Parisi and Sourlas[23] have shown that the asymptotic properties of LAs in  $d$  dimensions are the same as the critical properties of the Lee-Yang edge singularity (LYES) of the Ising model in  $d - 2$  dimen-

sions. For the directed LA problem, the dimensional reduction is  $d - 1$  [24]. The LYES problem has to do with the fact that ferromagnetic Ising models, besides exhibiting singular behaviour at the critical point  $T = T_c$ , in the presence of zero external magnetic field, show singular behaviour also at a critical value of imaginary magnetic field  $H = H_0(T)$  and for  $T \neq T_c$ . The magnetization has a branch point singularity of the form

$$M - M_0 \sim (H - H_0)^\sigma \quad (11)$$

where  $M_0$  is the magnetization at  $H_0$ . Consequently, the free energy  $F$  of the  $(d - 2)$ -dimensional Ising model has the same singular structure as that of the generating function of the  $d$ -dimensional undirected LA problem. From Eqs.(3) and (4), it follows that the LA generating function  $G(x)$  has a singularity of the form  $(x - x_c)^{\theta-1}$  where  $x_c = 1/\lambda$ . Since magnetization is the first derivative of the free energy  $F$  w.r.t. the magnetic field  $H$ ,  $F$  has a power-law singularity of the type (11) with the exponent  $\sigma + 1$ . From the equivalence of the free energy and the generating function in appropriate dimensions, one obtains

$$\theta(d) = \sigma(d - 2) + 2 \quad (12)$$

The Josephson scaling law (the hyperscaling relation) connects the singularity of the free energy  $F$  with the singularity of the correlation length  $\xi$ , ( $F \sim \xi^{-d}$ ). One thus obtains

$$\nu(d) = [\sigma(d - 2) + 1]/(d - 2) \quad (13)$$

Each undirected and unrooted LA of  $N$  sites gives rise to  $N$  distinct rooted site animals. Thus the animal number exponents, in the two cases, differ by 1. Thus, from (12) and (13), one gets

$$\theta = (d - 2)\nu \quad (14)$$

for rooted undirected animals. Similarly, one can show that

$$\theta = (d - 1)\nu_\perp \quad (15)$$

for rooted directed animals. The exponent  $\nu_\perp$  is associated with the radius of gyration of the directed animals perpendicular to the preferred direction



of growth. We have seen that the LA exponents  $\theta$ ,  $\nu$  are related to the LYES exponent  $\sigma$ . The value of  $\sigma$  can be calculated exactly for  $d = 0$  (point particle) and  $d = 1$ . Thus from Eqs.(12) and (13), the exponents  $\theta$ ,  $\nu$  can also be determined exactly in appropriate higher dimensions (upto  $d = 3$ ). The directed LA problem is exactly solvable in both 2d and 3d[25]. So exploiting the fact that directed animal exponents in  $d$  dimensions are related to the ordinary animal exponents in  $(d + 1)$  dimensions and to the LYES exponents in  $(d-1)$  dimensions,  $\theta$ ,  $\nu$  are exactly known for ordinary animals in  $d = 4$  and  $\sigma$ , the LY exponent, in  $d = 2$ . The results for  $\sigma(d)$ ,  $\theta(d)$ ,  $\nu(d)$  are:  $\sigma(0) = -1$ ,  $\sigma(1) = -1/2$ ,  $\sigma(2) = -1/6$ , for ordinary animals  $\theta(2) = 1$ ,  $\theta(3) = 3/2$ ,  $\theta(4) = 11/6$ ,  $\nu(3) = 1/2$ ,  $\nu(4) = 5/12$  and for directed animals  $\theta(2) = 1/2$ ,  $\theta(3) = 5/6$ ,  $\nu_{\perp}(2) = 1/2$ ,  $\nu_{\perp}(3) = 5/12$ .

To study dimensional reduction in the spiral animal problem, Bose et al[10] have considered only spiral trees. Both exact enumeration and MC simulation have been performed. The spiral trees considered are rooted and the rotational constraint is operative only in the xy plane. The radius of gyration has two components  $R_{s,pl}$  in the xy plane and  $R_{s,\perp}$  in the direction perpendicular to the xy plane. The numerical data obtained are consistent with the following results:

$$\begin{aligned}\theta_0 &= (d-4) \nu_{0,pl} \quad (d=2) \\ \theta_0 &= (d-4) \nu_{0,\perp} \quad (d>2)\end{aligned}\tag{16}$$

Eq.(16) shows that a dimensional reduction by 4 occurs in the spiral animal problem. The dimensional reduction by the factor two, in the case of ordinary animals, occurs due to a hidden supersymmetry[23, 26]. The first few applications of supersymmetry in condensed matter and statistical physics include the following problems: the random field model, the linear polymers (SAWs on a lattice), the branched polymers (LAs) and electron localization. These models can be suitably recast into forms which manifest supersymmetry. Introduction of an effective supersymmetry simplifies technically complicated calculations. Also, as in the cases of branched polymers and random field models, which are closely related, the supersymmetry can be shown to lead to an effective reduction in the number of degrees of freedom. For the directed animal problem, the dimensional reduction by 1 occurs because the disorder or cellular automaton condition is satisfied. Field theories have been formulated for both ordinary and directed animal problems, specially,

with the view to understand the mechanism of dimensional reduction. For spiral LAs, a complete theory is yet to be worked out. A simple example of reduction of effective dimensionality due to rotational constraint, is provided by the quantum mechanical motion of a charged particle in a uniform magnetic field. If the field is perpendicular to the xy plane, then the degrees of freedom in this plane get quantized. The resulting discrete spectrum has no contribution to the density of states of low energy excitations. This leads to a reduction by 2 in the effective dimensionality. One can argue, in analogy, that for the spiral animal problem also, the rotational constraint is responsible for a dimensional reduction by 2. A further reduction by 2 occurs due to the conventional Parisi-Sourlas mechanism.

Recently, the problem of rooted spiral site trees embedded in a triangular lattice has been studied by exact enumeration[27]. It will be of interest to verify whether the dimensional reduction by 4 occurs in this case also. The universality of the exponents  $\theta$  and  $\nu$  imply that they have the same values as long as the dimension d of the underlying lattice is the same. Also, the values remain unchanged if one considers bond LAs instead of site LAs. These facts are well-established for both the undirected and directed LA problems. Preliminary results in the case of the spiral LA problem, however, indicate that the values of  $\theta$  and  $\nu$  are different for the square and triangular lattices. If the result is proved to be true, then one has an example of the breakdown of universality in the case of the LA problem.

We next consider the configurational statistics of spiral site LAs with  $c$  ( $c = 0, 1, 2, \dots$ ) number of loops. The corresponding growth parameter and the exponents are  $\lambda_c$ ,  $\theta_c$  and  $\nu_c$  respectively. The number of loops  $c$  in an animal of  $s$  sites has been determined through the relations:

$$b = 1/2 \sum_{i=1}^z i q(i) \quad , c = b - s + 1 \quad (17)$$

where  $b$  is the number of bonds in the animal,  $z$  is the coordination number of the lattice and  $q(i)$  is the number of sites in the animal which have  $i$  nearest-neighbour occupied sites. In the case of undirected and directed LAs,  $\lambda_c$  and  $\nu_c$  are independent of  $c$  and equal to  $\lambda_0$  and  $\nu_0$ , the respective values for trees. The animal number exponent  $\theta_c$  is related to that for trees ( $\theta_0$ ) through the relation [22, 28, 29]

$$\theta_c = \theta_0 - c \quad (18)$$

A rigorous proof of (18) has been given for undirected weakly-embeddable animals ( bond animals) in the square lattice[30]. Universality demands that the same relation be true for strongly-embeddable (site) animals. For spiral LAs, no rigorous result is available but calculations based on exact enumeration data suggest the relation

$$\theta_c = \theta_0 - \alpha c \quad (19)$$

where  $\alpha = 1.5 \pm 0.2$ . Whittington et al [28] have derived the inequality

$$\theta_c \geq \theta_{c+1} \geq \theta_c - 1 \quad (20)$$

The inequality is derived from another inequality involving LA numbers

$$g_{s-3,c} \leq g_{s,c+1} \leq 2ds g_{s,c} \quad (21)$$

where  $g_{s,c} \sim \lambda_c^s s^{-\theta_c}$ . For spiral site animals, an inequality similar to the first half of the inequality in (21) can be proved[18]. Let the vertices or sites of the spiral animals have coordinates  $(x_i, y_i)$ ,  $i=1,2,\dots,n$ . Following Whittington et al[28], the top (bottom) vertex is defined as the vertex having maximum (minimum) x coordinate and, in case of ambiguity, the vertex in this subset having maximum (minimum) y coordinate. Consider any c-loop animal belonging to the set  $W_{s,c}$  of animals with s sites and c loops. The number of animals is  $g_{s,c}$ . Let t be the top vertex of the animal with coordinates  $(x_t, y_t)$ . The top vertex can be approached in three ways: (i) from the vertex  $(x_t - 1, y_t)$  if it is occupied, (ii) from the vertex  $(x_t, y_t - 1)$  if it is occupied, (iii) from both the vertices  $(x_t - 1, y_t)$  and  $(x_t, y_t - 1)$  if both are occupied.

In cases (ii) and (iii), add four vertices  $v_1, v_2, v_3, v_4$  with coordinates  $(x_t + 1, y_t)$ ,  $(x_t + 1, y_t - 1)$ ,  $(x_t + 2, y_t)$  and  $(x_t + 3, y_t)$  respectively. For lattice site animals, addition of a new site implies that the bonds between this site and its nearest occupied neighbours automatically exist. Addition of four new sites leads to an increase in the number of bonds by five. The number of loops therefore increases by one. The new animal obtained is also spirally connected and so belongs to the set  $W_{s+4,c+1}$  of animals with c+1 loops. In case (i), there are two possibilities, either the vertex  $(x_t, y_t - 1)$  is occupied or unoccupied. If the first possibility is true, add four vertices with the same coordinates as in the cases of (ii) and (iii) to get a spiral animal of  $s + 4$  sites and c+1 loops. If the second possibility is true, add vertices with coordinates

$(x_t + 1, y_t), (x_t + 2, y_t), (x_t + 1, y_t - 1)$  and  $(x_t + 2, y_t - 1)$  generating a spiral animal of  $s + 4$  sites and  $c + 1$  loops. Thus for each animal belonging to the set  $W_{s,c}$  of animals, an animal belonging to the set  $W_{s+4,c+1}$  can be generated ,i.e.,  $g_{s,c} \leq g_{s+4,c+1}$  or,  $g_{s-4,c} \leq g_{s,c+1}$ .

The proof given by Whittington et al[28] for the second half of the inequality fails in the case of spiral animals. For undirected weakly embeddable animals, an upper limit to  $g_{s,c}$  is  $2dsg_{s,c-1}$  as there are  $s$  vertices and at each vertex an edge can be added in  $2d$  ways, addition of an edge (bond) implying an increase in the number of loops by 1. Thus  $g_{s,c} \leq 2dsg_{s,c-1}$ , or,  $g_{s,c+1} \leq 2dsg_{s,c}$ , the second half of the inequality in (21), is obtained. In the case of spiral lattice animals, animals with  $c$  loops can be generated not only from spiral animals with  $c-1$  loops but also from undirected animals with  $c-1$  loops, which on the addition of an edge( bond) become spirally connected with  $c$  loops. Thus a simple relation like  $g_{s,c} \leq 2dsg_{s,c-1}$  cannot be written down for spiral lattice animals.

For spiral LAs, no rigorous results are available. This is in contrast to the case of directed LAs. In this context, we mention a directed compact site LA problem on the  $d$ -dimensional hypercubic lattice[31]. It has been rigorously established that the model is equivalent to the (i) infinite-state Potts model and (ii) the enumeration of  $(d-1)$ -dimensional restricted partitions of an integer. Thus, the directed compact LA problem can be solved exactly in  $d = 2,3$  using known solutions of the enumeration problem mentioned. Also, knowledge of the infinite-state Potts model solution leads to a conjectured limiting form, for  $d \geq 3$ , of the generating function of restricted partitions. The latter problem is still unsolved in number theory. The examples of SSAW and the directed compact site LA problem show that the well-known mathematical theory of partition of integers can be used to derive rigorous results for lattice-statistical models.

## IV. Spiral site percolation

Santra et al[32, 33] have formulated a new type of percolation model known as spiral percolation in which a rotational constraint is operative due to which each step in a percolation path is either in the forward direction or in a specific rotational direction, say, clockwise. Consider spiral site percolation on a lattice in  $2d$  of size  $L \times L$ . The spiral percolation threshold is

determined by the binary search method [3]. One starts from a central site of the lattice called the origin. Initially, from the origin, one can proceed in any one of the four possible directions. The nearest-neighbour (n.n.) sites in these directions are occupied with probability  $p$  by using a random number generator. With each occupied site a variable  $JVISIT(IV, INOW)$  is associated.  $INOW$  is the site index and  $IV$  the direction index. The sites of the lattice are numbered according to a particular sequence; the site index is the number associated with a site. A site can be reached from four directions, south, west, north and east. The corresponding direction indices are 1, 2, 3 and 4 (Figure 5(a)). The rotational constraint implies the following: if a site has direction index 1, then occupy with probability  $p$ , only those of the n.n.s which are towards the north and east of the site. Initially, the  $JVISIT$  variable is assigned the value zero for all sites. As soon as a site is occupied, the corresponding  $JVISIT$  variable is given the value  $IV$  where  $IV$  is the direction index corresponding to the direction from which the site is occupied. All growing sites are put on a list and the walk-search is carried out for each. The growth of a cluster of occupied sites stops only when all the perimeter sites are unavailable for occupation. Figure 5(b) shows a typical cluster grown obeying the rotational constraint. Due to the nature of the constraint, loops are an essential feature of the growing spirally connected cluster. In the computer algorithm, the possibility of loop formation while growing a cluster is taken care of in the following manner. Refer to Figure 5(b). The site  $i$  is the origin. In the first step when  $j$  is occupied,  $JVISIT(i, j) = 1$ . Next time  $j$  is approached (from site  $m$ , say), the computer algorithm checks whether  $JVISIT(4, j)$  is zero. If it is non-zero then the site  $j$  has been approached from the east previously and so cannot be occupied again. For the particular cluster in Figure 5(b), since  $JVISIT(4, j)$  is zero, the site  $j$  is reoccupied and  $JVISIT(4, j)$  assigned the value 4. Thus loop formation and continuation of cluster growth are possible.

Following the binary search method, one starts growing a cluster with a particular value of  $p$ , say  $p_0$ . If the cluster grown spans (does not span) the lattice in either the east-west or north-south direction,  $p_0$  is decreased (increased) by a small amount. The same random number sequence is then used to get estimates  $p_1(L)$  and  $p_2(L)$  which bound an interval containing the true threshold value  $p_c(L)$ . By successive binary chopping of this interval one can determine  $p_c(L)$  with a specified accuracy. The whole process is then repeated  $N$  times ( $N \times L \times L$  is of the order  $(10^6 - 10^7)$ ) using different

random number sequences. The average value  $\langle p_c(L) \rangle$  of all the estimates obtained is taken as an estimate for the percolation threshold.

We now describe the scaling behaviour of the percolation clusters in the vicinity of the percolation threshold. In the case of undirected percolation, the most widely used method of calculating the scaling behaviour is to fill up a large lattice by clusters of various sizes  $s$  with site occupation probability  $p$ [3]. The cluster size distribution is given by  $n_s(p)$ , the number of clusters of size  $s$  per site of the lattice. The probability that a site belongs to a cluster of size  $s$  is  $sn_s(p)$ . The probability that an arbitrary site belongs to any cluster is equal to the probability that it is occupied. Thus

$$\sum_s s n_s(p) = p \quad (p < p_c) \quad (22)$$

$$\sum_s s n_s(p) + P_\infty(p) = p \quad (p > p_c) \quad (23)$$

The sums in (22) and (23) run over all possible finite cluster sizes.  $P_\infty(p)$  is the probability that an arbitrary site (occupied or not) belongs to the infinite cluster. The percolation probability  $P(p)$  is defined as the probability that an occupied site belongs to the infinite cluster, i.e.,

$$P(p) = P_\infty / p = 1 - \sum_s s n_s(p) \quad (24)$$

Let  $W = (sn_s) / (\sum_s sn_s)$  be the probability that the cluster to which an arbitrary occupied site belongs contains exactly  $s$  sites. The average cluster size  $S_{av}$  is then given by

$$S_{av} = \sum_s s W_s = \sum_s (S^2 n_s) / (\sum_s sn_s) \quad (25)$$

The linear size of the finite clusters, below and above  $p_c$ , is characterised by the correlation length  $\xi$ . The correlation length is defined as the mean distance between two sites on the same finite cluster. As the site occupation probability  $p$  reaches the percolation threshold  $p_c$ , the various moments of the cluster size distribution  $n_s(p)$  given by

$$\sum_s s^k n_s(p), \quad k = 0, 1, 2, \dots \quad (26)$$

(the prime denotes that the largest cluster is excluded from the sum) become singular with characteristic critical exponents. The critical exponents  $\alpha, \beta, \gamma, \delta, \nu$  are defined through the relations

$$k = 0: \quad \left( \sum_s' n_s \right)_{sing} \sim |p - p_c|^{2-\alpha} \quad (27)$$

$$k = 1: \quad P(p) \propto \left( \sum_s' s n_s \right)_{sing} \sim (p - p_c)^\beta \quad (28)$$

$$k = 2: \quad S_{av} \propto \sum_s' s^2 n_s \sim |p - p_c|^{-\gamma} \quad (29)$$

$$\xi = |p - p_c|^{-\nu} \quad (30)$$

$$\sum s n_s(p_c) (1 - e^{-hs}) \sim h^{1/\delta} \quad (31)$$

The subscript ‘sing’ refers to the leading non-analytic contribution. The above equations are valid in the limit in which the fictitious field  $h$  and the quantity  $|p - p_c|$  both go to zero.

We now consider the case of spiral site percolation. The scaling behaviour of clusters in the critical region is studied following the single-cluster growth method in which clusters are grown singly starting from a fixed origin instead of filling up the whole lattice by clusters of various sizes. The computer algorithm has already been described. The cluster size distribution is now defined as

$$P_s(p) = N_s / N_{tot} \quad (32)$$

where  $N_s$  is the number of clusters of size  $s$  in a total number  $N_{tot}$  of clusters generated. The various moments of  $P_s(p)$ ,  $\sum_s' s^k P_s(p)$  becomes singular as  $p \rightarrow p_c$ . The prime in the summation symbol indicates that the largest cluster is to be left out of the sum. The average cluster size  $\chi$  is given by

$$\chi \sim \sum_s' s P_s(p) \quad (33)$$

which diverges as  $\chi \sim |p - p_c|^{-\gamma}$  as  $p \rightarrow p_c$ . In the single cluster growth method, the cluster configurations are rooted at the origin and the first, not the second, moment of the cluster size distribution defines the exponent  $\gamma$ . In fact, any exponent which corresponds to the  $k$ th moment of the cluster size

distribution in the case of the lattice-filling method, is obtained from the  $(k-1)$ th moment, one order less, in the case of the single cluster growth method. In the case of directed and spiral percolation, where there is a directionality constraint on the percolation process, the single cluster growth method is the appropriate one for the study of critical behaviour.

The percolation transition is a second-order phase transition and exhibits the critical phenomena characteristic of second-order thermodynamic phase transitions like liquid-gas and paramagnet-ferromagnet transitions. The major characteristic feature, which we have already discussed, is that different cluster-related quantities exhibit power-law behaviour as  $p \rightarrow p_c$ . One of these, the percolation probability  $P(p)$  (Eq.(24)) serves as the order parameter of the transition. The order parameter has a non-zero value in one phase ( $p > p_c$ ) and is zero in the other phase ( $p < p_c$ ). As in the case of thermodynamic phase transitions, the critical behaviour is universal, i.e., the magnitude of the critical exponents depends only on the dimensionality of the lattice and is the same for both site and bond percolation. The critical exponents are not independent (only two are so) and one can write down ‘scaling’ relations connecting different critical exponents. The scaling relations can be determined on the basis of the scaling hypothesis according to which in the vicinity of  $p = p_c$ , the cluster-related quantities become generalised homogeneous functions (GHF). A function  $F(x,y)$  of two variables is a GHF if it satisfies the property

$$F(x, y) = x^A f(y/x^B) \quad (34)$$

where the function  $f$  is the appropriate scaling function and is the function of a single variable. The form (34) usually holds true when both the variables  $x$  and  $y$  tend to zero. The definition (34) of a GHF can be generalised to more than two variables. A second-order thermodynamic phase transition has the feature that fluctuations occur at all length scales, i.e., the correlation length goes to infinity. In the case of percolation transition also, the correlation length goes to infinity. The infinite percolation cluster is a self-similar object with fractal dimension less than the Euclidean dimension of the space in which the cluster is embedded.

We now describe the approximate methods for calculating the critical exponents and determining the scaling behaviour of the cluster-size distribution function. The methods normally used are Monte Carlo (MC) simulation,



finite-size scaling, series-expansion and renormalization group. We consider the case of spiral site percolation on the square and triangular lattices and describe the results obtained by Santra and Bose[32, 33]. In MC simulation, a particular lattice size is considered. The value of the percolation threshold  $p_c$  is determined by the binary search method. Ten thousand cluster are generated by the single cluster growth method. The growth of a cluster is stopped when there is no further site available for occupation. The quantities, the average cluster size  $\chi$  (Eq.33), the second moment  $\chi'$  of the cluster size distribution  $P_s(p)$  and the correlation length  $\xi$  are determined as a function of  $|p - p_c|$ . As the site occupation probability  $p$  tends towards the percolation threshold,  $\chi$ ,  $\chi'$  and  $\xi$  diverge with the exponents  $\gamma, \gamma'$  and  $\nu$ . We first quote the results for the square lattice. The value of  $p_c$  is  $p_c = 0.711 \pm 0.001$ . The critical exponent  $\gamma$  is obtained from the slope of  $\log \chi$  versus  $\log |p - p_c|$  and is given by  $\gamma = 2.19 \pm 0.07$ . The exponents  $\gamma'$  and  $\nu$  are  $\gamma' = 4.51 \pm 0.16$  and  $\nu = 1.16 \pm 0.01$ . The exponent  $\nu$  can also be determined from the scaling relation  $\nu = (\gamma' - \gamma)/2$  as  $\nu = 1.18 \pm 0.23$ . This value is in agreement with the value obtained through direct measurement. For the triangular lattice,  $p_c = 0.667 \pm 0.001$ ,  $\gamma = 2.079 \pm 0.062$ ,  $\gamma' = 4.376 \pm 0.199$  and  $\nu = 1.012 \pm 0.025$ .

True critical behaviour occurs only in the limit of infinitely large lattices. An estimate of the critical exponents can, however, be obtained from the studies of finite systems by assuming the finite-size scaling hypothesis[3] which leads to the formula

$$A = L^{-x/\nu} F[(p - p_c) L^{1/\nu}] \quad (35)$$

where  $A$  is a quantity which becomes critical,  $A \sim |p - p_c|^x$  as  $p \rightarrow p_c$ . The function  $F$  is a suitable scaling function. At  $p = p_c$ , the quantity  $A$  varies as  $L^{-x/\nu}$ . This result can be used to determine the exponents  $\gamma/\nu$ ,  $\gamma'/\nu$  by calculating the first and second moments  $\chi$  and  $\chi'$  respectively, of the cluster size distribution. The percolation threshold  $p_c = \langle p_c(L) \rangle$ , the average being taken over a large number of estimates of  $p_c$  for a  $L \times L$  lattice. The largest cluster spanning the lattice is of size  $S_L$  and is a fractal with fractal dimension  $d_f$  defined by

$$S_L \sim L^{d_f} \quad (36)$$

The fractal dimension  $d_f$  can again be written as

$$d_f = d - \beta/\nu \quad (37)$$

where  $\beta$  is the exponent associated with the order parameter. From (36), the fractal dimension  $d_f$  can be determined and from (37) putting  $d = 2$ , the value of  $\beta/\nu$  can be calculated. The measurement of various quantities is done for lattices of various sizes. The slope of the straight line  $\log S_L$  versus  $\log L$  gives  $d_f = 1.965 \pm 0.009$  and so  $\beta/\nu = 0.043 \pm 0.009$ . From (35), the plot of  $\log A$  versus  $\log L$  at  $p = p_c$  gives the exponent  $x/\nu$ . Thus for  $A = \chi$ , the average cluster size, the exponent  $\gamma/\nu = 2.01 \pm 0.06$ . For  $A = \chi'$ , the second moment of the cluster size distribution, the exponent  $\gamma'/\nu = 4.05 \pm 0.13$ . For the triangular lattice, the various quantities have been determined as  $d_f = 1.965 \pm 0.008$ ,  $\beta/\nu = 0.035 \pm 0.008$ ,  $\gamma/\nu = 1.867 \pm 0.028$  and  $\gamma'/\nu = 3.829 \pm 0.062$ .

We now describe the method of series expansion. The probability  $p$  that the origin from which clusters grow is occupied can be written as a sum over all finite clusters that start from it (for  $p \leq p_c$ ), i.e.,

$$p = \sum_{s,t} g_{st} p^s (1-p)^t = \sum_s p^s D_s(q), \quad q = 1-p \quad (38)$$

where  $g_{st}$  is the number of clusters or LAs of  $s$  sites and  $t$  perimeter sites and  $D_s(q)$ 's are the perimeter polynomials. The animals are rooted at the origin. The average cluster size  $\chi$  is the first moment of the cluster size distribution.

$$\chi = \sum_{s,t} s g_{st} p^s (1-p)^t \sim |p - p_c|^{-\gamma} \quad (39)$$

as  $p \rightarrow p_c$ . The clusters rooted at the origin obey the same rotational constraint as in the percolation process. The spiral LAs, as already mentioned in Section III, have been extensively studied by Bose et al [9, 10, 18]. The major focus in these studies has been on spiral site LAs with no fixed origin. If the origin is not kept fixed, the number of perimeter sites is dependent on the position of the origin. In spiral percolation, the percolation clusters are rooted at the origin so the spiral LAs in the series-expansion method have to be rooted, i.e., have a fixed origin. Now each distinct LA configuration has a unique value for the number of perimeter sites. The rooted spiral site LAs on the square lattice have been enumerated exactly by Santra and Bose[33] for size upto 13. Thus, series expansion for the average cluster size  $\chi$  (eq.(39)) is exactly known, when expanded in powers of  $p$ , upto the term containing the power  $p^{13}$ . A standard trick [33] enables one to extend the series by one more power. Thus the coefficients in the expansion of  $\chi = 1 + \sum_r b_r p^r$  (a common

factor of  $p$  has been taken out), are exactly known for  $r = 1$  to 13. As  $p \rightarrow p_c$ ,  $\chi$  has the power-law behaviour  $\chi \sim (p_c - p)^{-\gamma} = p_c^{-\gamma} (1 - p/p_c)^{-\gamma}$ . On binomial expansion, the ratio of coefficients  $b_{k+1}/b_k = 1/p_c (1 + (\gamma - 1)/(k + 1))$ . The plot  $b_{k+1}/b_k$  versus  $1/(k+1)$  should be a straight line. The intercept of the line on the y-axis gives  $1/p_c$  and from the slope, knowing  $p_c$ , the exponent  $\gamma$  can be determined. A more sophisticated method of obtaining the value of  $\gamma$  is that of Padé approximants. Using this method, the value of  $\gamma$  for spiral site percolation on the square lattice has been obtained as  $\gamma = 2.167 \pm 0.004$ . For lack of a sufficiently long series, the series-expansion method has not been applied to the triangular lattice. The series-expansion method can be applied to generate the series for other percolation-related quantities and thereby obtain the values of the associated exponents.

We now discuss the scaling hypothesis for percolation clusters. From Eq.(34), one finds that if the function  $G(z) = F(x, y)/x^A$  is plotted as a function of  $z = y/x^B$ , all the data (for different values of  $x$ ) fall on a single curve described by the function  $f(z)$ . On the other hand, if Eq.(34) were not true, the data, for different values of  $x$ , fall on separate curves. The collapse of data on a single curve serves as a verification of the scaling hypothesis. The cluster size distribution function for sufficiently large  $s$  has the scaling form in the critical region given by[33]

$$P_S(p) = s^{-\tau+1} f[(p - p_c) s^\sigma] \quad (40)$$

where both  $p - p_c$  and  $1/s$  go to zero as  $p \rightarrow p_c$ . The exponents  $\tau$  and  $\sigma$  are related to the exponents  $\gamma$  and  $\beta$  through the relations

$$\gamma = (3 - \tau)/\sigma, \beta = (\tau - 2)/\sigma \quad (41)$$

A verification of the scaling function form (40) is possible by plotting  $P_s(p)/P_s(p_c)$  against  $(p - p_c)s^\sigma$ . If the scaling form is true then, for sufficiently large clusters and for different values of  $p$ , the data should collapse onto a single curve. For the square and triangular lattices, the scaling form (Eq.(40)) for spiral site percolation has been verified with  $\sigma = 0.446$  (square lattice) and  $\sigma = 0.473$  (triangular lattice).

The values of the critical exponents obtained for spiral site percolation in 2d are different from the values of critical exponents in the case of undirected percolation. Spiral percolation is similar in nature to directed percolation, since for both the models a directional constraint is operative. In the first

case, the directional constraint is rotational in nature and in the second case percolation occurs only in certain specific directions. Dhar and Barma[34] have studied directed site percolation on the square lattice using MC simulation. A comparison with their results shows that the average cluster size exponent  $\gamma = 2.19 \pm 0.03$  (directed percolation) is the same as that obtained in the case of spiral percolation,  $\gamma = 2.19 \pm 0.07$ , using MC simulation. Thus the average cluster size diverges with the same exponent irrespective of the nature of the external constraint. One crucial difference between spiral and directed percolation is that in the first case, percolation clusters grow isotropically whereas in the second case, the clusters grown are anisotropic in nature. For the first case, there is thus only one correlation length which diverges with the exponent  $\nu$  as  $p \rightarrow p_c$ , whereas, in the second case, there are two correlation lengths, one parallel and the other perpendicular to the preferred direction, which diverge with the exponents  $\nu_{\parallel}$  and  $\nu_{\perp}$  respectively as  $p \rightarrow p_c$ .

One important quantity in the percolation problem is the cluster external perimeter or ‘hull’ of the large clusters. The hull of a cluster is the continuous path of occupied sites at the external boundary of the cluster. The hull has a significance of its own apart from being a part of the percolation cluster. Sapoval et al[35] have shown that the diffusion front arising out of diffusion from a source has a fractal structure that is related to the hull of percolation clusters. The percolation cluster hull in the case of undirected percolation exhibits scaling behaviour characterised by critical exponents which have values different from those of analogous quantities in the case of percolation clusters. Santra and Bose [36] have studied the scaling behaviour of the percolation hull of large clusters in the case of spiral site percolation on the square and triangular lattices. The scaling behaviour is found to be different from that of hull in the case of undirected percolation. In the latter case, Saleur and Duplantier[37] have proved that the fractal dimension,  $d_H$ , of the hull is given by

$$d_h = 1 + 1/\nu \quad (42)$$

where  $\nu$  is the correlation length exponent. Eq.(42) is an exact result. A similar relation cannot be proved in the case of spiral site percolation.

## V. Concluding Remarks

The rotational constraint, we have seen, has a non-trivial effect on the statistics of lattice models like SAW, LA and percolation. The undirected SAW and LA problems have been extensively studied and some fairly rigorous results are available. For undirected percolation in 2d, the values of  $p_c$  are known exactly in some cases. The critical exponents are, through some exact mappings, conjectured to be known exactly[38]. For the directed SAW, LA and percolation problems, many exact/analytical results are available. In the presence of a rotational constraint, however, the only rigorous results that are known are for the SSAW model. The spiral LA and spiral percolation problems have been studied through numerical methods. Derivation of numerical results for the models is a challenge for both mathematicians and physicists. The computational methods in the case of spiral models are also more difficult to implement than in the case of undirected and directed models.

Lattice models have extensive applications in all branches of science. The SAW model describes a correlated walk, i.e., a walk with memory. The knowledge gained from the study of the model has been found to be useful in problems like correlations in nucleotide sequences[39] and the folding of proteins[40]. Several examples of the various applications of the lattice models can be found in the Refs.[ 1-5]. Examples of the spiral structures and the rotational constraint can be found in Ref. [41]. A few examples are: spiral galaxies, the pattern of shoot arrangement in plants, scales on a pineapple or on a pine cone, the Belousov-Zhabotinsky reaction, plasma in a stochastic magnetic field, polymers with spiral structure, bacterial colonies which exhibit chiral morphology[42] (the colony consists of twisted branches all with the same handedness) etc. It is to be hoped that further studies will be undertaken to understand the effect of rotational constraint on the properties of model systems.

### Acknowledgement

I thank Asimkumar Ghosh for help in preparing the manuscript.

## References

- [1] P.G.de Gennes, Scaling Concepts in Polymer Physics, (Cornell University Press, Ithaca, New York, 1979).
- [2] H.E.Stanley and N.Ostrowsky (eds.), On Growth and Form: Fractals and Non-Fractal Patterns in Physics, (Martinus Nijhoff Publishers, Dordrecht, The Netherlands, 1986).
- [3] D.Stauffer, Introduction to Percolation Theory (Taylor and Francis, London, 1985).
- [4] A.Bunde and S.Havlin (eds.), Fractals and Disordered Systems, (Springer-Verlag, Berlin, 1991).
- [5] D.Stauffer,Phys.Rep. 54,1 (1979).
- [6] F.Family, J.Phys.A : Math.Gen. 15, L583 (1982).
- [7] V.Privman, J.Phys.A: Math.Gen. 16, L571 (1983).
- [8] T.C.Li and Z.C.Zhou, J.Phys.A: Math.Gen. 18, 67(1985).
- [9] I.Bose and P.Ray, Phys.Rev.B 35, 2071(1987); I.Bose,P.Ray and S.Mukhopadhyay, J.Phys.A: Math.Gen. 21, L979 (1988).
- [10] I.Bose, P.Ray and D.Dhar,J.Phys.A: Math.Gen. 21,L219 (1988).
- [11] H.W.J. Blöte and H.J.Hilhorst, J.Phys.A: Math. Gen. 17, L111 (1984).
- [12] A.J.Guttman and N.C.Wormald, J.Phys.A: Math.Gen. 17, L271 (1984).
- [13] A.J.Guttman and M. Hirschhorn, J.Phys.A: Math.Gen. 17, 3613 (1984).
- [14] K.Y.Lin, J.Phys.A: Math. Gen. 18, L145 (1985).
- [15] G.H.Hardy and S.Ramanujan, Proc. London Math.Soc. (2) 17, 75 (1918).
- [16] G.S.Joyce, J.Phys.A: Math.Gen. 17, L463 (1984).

- [17] J.L.Martin in Phase Transitions and Critical Phenomena, ed. by C.Domb and M.S.Green (Academic, London, 1974), vol.III, p.97.
- [18] S.B.Santra and I.Bose, J.Phys.A:Math.Gen. 22,5043 (1989).
- [19] T.C.Lubensky and J.Isaacson, Phys.Rev.A 20, 2130 (1979).
- [20] F.Family, J.Phys.A: Math.Gen. 13, L325 (1980).
- [21] M.Daoud and J.F.Joanny, J.Physique 42, 1359 (1981).
- [22] J.A.M.S. Duarte, J.Physique Lett. 46, L523 (1985).
- [23] G.Parisi and N.Sourlas, Phys.Rev.Lett. 46, 871(1981).
- [24] H.E.Stanley, S.Redner and Z.R.Yang, J.Phys.A: Math.Gen. 15, L569 (1982).
- [25] D.Dhar, Physica 140A, 210 (1986).
- [26] N.Sourlas, Physica D 15, 115 (1985).
- [27] S.B.Santra, J.Phys.France 5, 1573 (1995).
- [28] S.G.Whittington, G.M.Torrie and D.S.Gaunt, J.Phys.A: Math.Gen. 16, 1695 (1983).
- [29] P.M.Lam, Phys.Rev. A 35, 349 (1987).
- [30] C.E.Soteros and S.G.Whittington, J.Phys.A: Math.Gen. 21, 2187 (1988).
- [31] F.Y.Wu, G.Rollet, H.Y. Huang, J.M.Maillard, C.K.Hu and C.N.Chen, Phys.Rev.Lett. 76, 173 (1996).
- [32] S.B.Santra and I.Bose, J.Phys.A: Math.Gen. 24,2367 (1991).
- [33] S.B.Santra and I.Bose, J.Phys.A: Math.Gen. 25, 1105 (1992).
- [34] D.Dhar and M.Barma, J.Phys.C: Solid State Phys. 14, L1 (1981).
- [35] B.Sapoval, M.Rosso and J.F. Gouyet, J.Physique Lett. 46, L149 (1985).

- [36] S.B.Santra and I.Bose, J.Phys.A: Math.Gen. 26, 3963 (1993).
- [37] H.Saleur and B.Duplantier, Phys.Rev.Lett. 58, 2325 (1987).
- [38] M.B.Isichenko, Rev.Mod.Phys. 64, 961 (1992).
- [39] C.K.Peng, S.V.Buldyrev, A.L.Goldberger, S.Havlin, F.Sciortino, M.Simons and H.E.Stanley, Nature 356, 168 (1992).
- [40] H.S.Chan and K.A.Dill, Physics Today, February issue, p.24 (1993).
- [41] I.Hargittai and C.A.Pickover (eds.), Spiral Symmetry, (World Scientific, singapore, 1992).
- [42] E.Ben-Jacob, I.Cohen, O.Shochet, A.Tenenbaum, A.Czirók and T.Vicsek, Phys.Rev.Lett. 75, 2899 (1995).



## Figure Captions

**Fig.1** A spiral self-avoiding walk with an outward spiralling part and an inward spiralling part; 'O' denotes the origin.

**Fig.2** Three different spiral self-avoiding walks with origin O and end-point N. The broken line divides the walk into two parts.

**Fig.3** (a) A partition of the number 12 into the integers 4,4,2 and 2. (b) the spiral self-avoiding walk corresponding to the set of points in (a).

**Fig.4** A spiral lattice animal of 10 sites on a square lattice grown from the origin X.

**Fig.5** (a) Direction indices of a site corresponding to the four different directions from which the site can be reached, (b) an example of a spiral site cluster on the square lattice. The arrows on the bonds indicate the allowed spiral directions of flow from site i.

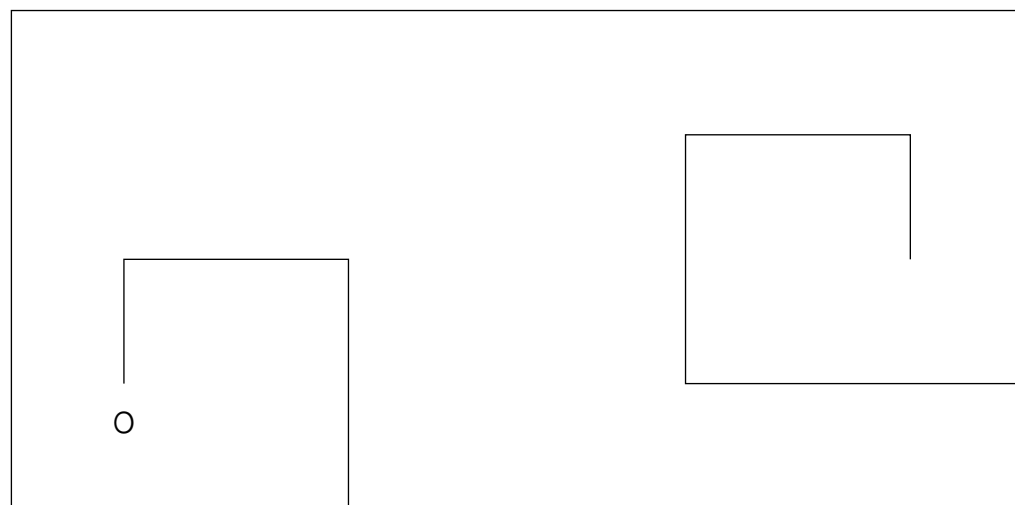


Figure 1

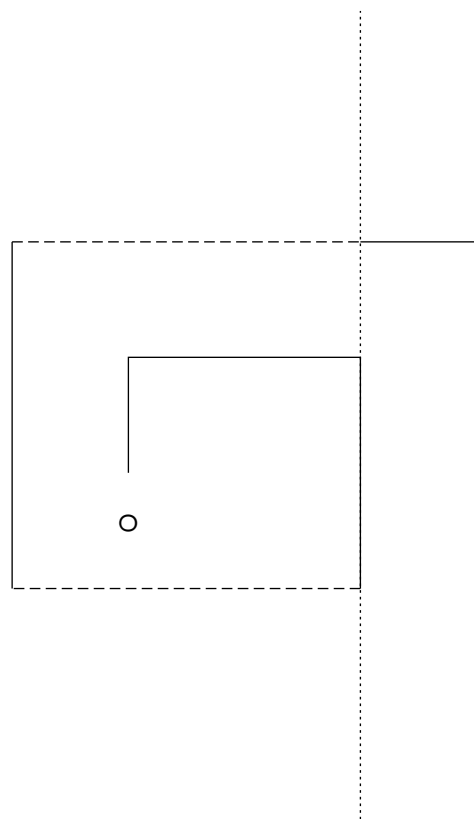


Figure 2(a)

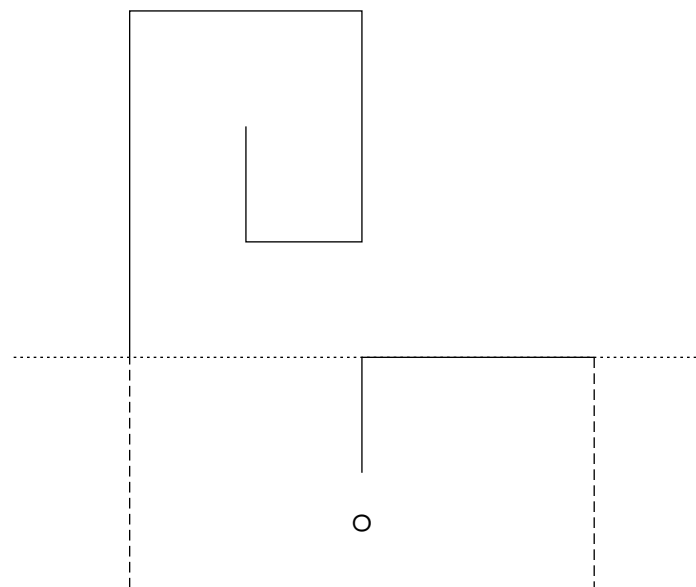
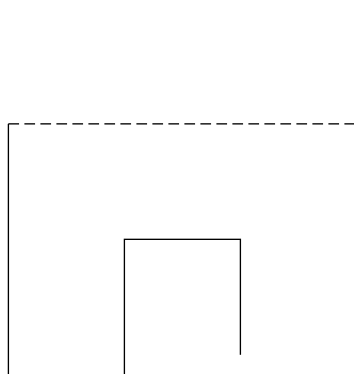


Figure 2(b)



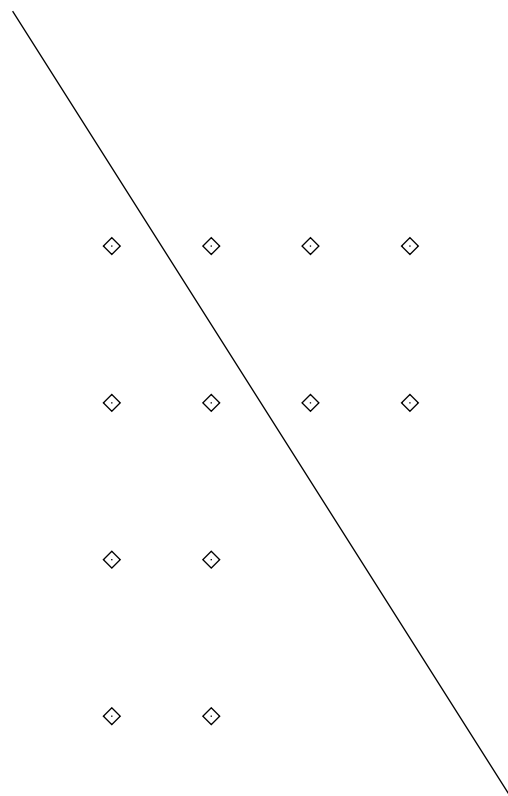


Figure 3(a)

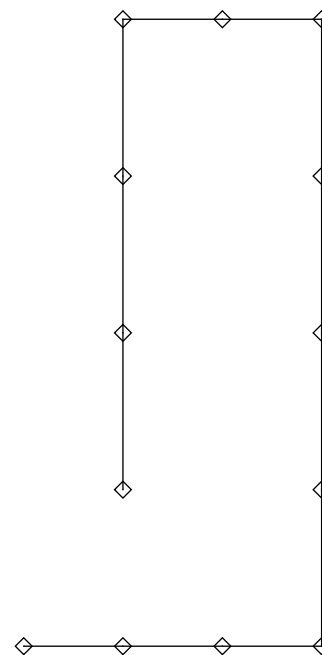


Figure 3(b)

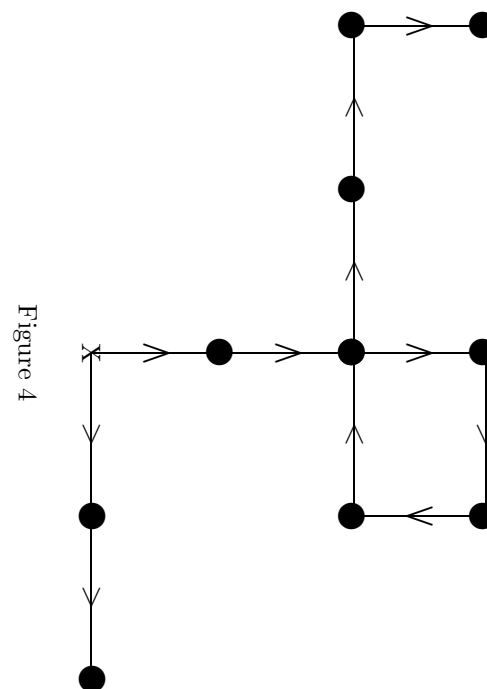


Figure 4

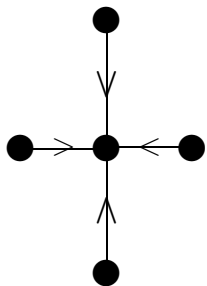


Figure 5(a)

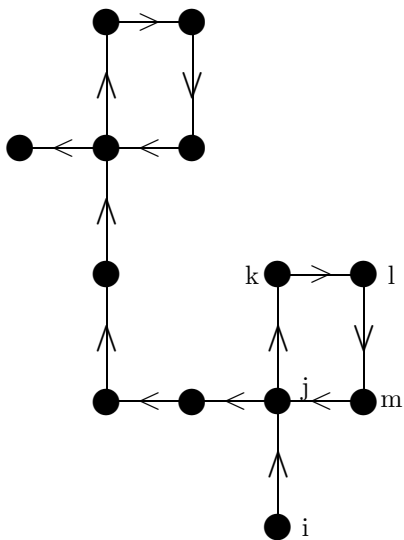


Figure 5(b)